

# Neutron Star vs Quark Star in the Multimessenger Era

Zheng Cao<sup>1</sup> and Lie-Wen Chen<sup>1,\*</sup>

<sup>1</sup>*School of Physics and Astronomy, Shanghai Key Laboratory for Particle Physics and Cosmology, and Key Laboratory for Particle Astrophysics and Cosmology (MOE), Shanghai Jiao Tong University, Shanghai 200240, China*

(Dated: September 1, 2023)

Neutron stars (NSs) which could contain exotic degrees of freedom in the core and the self-bound quark stars (QSs) made purely of absolutely stable deconfined quark matter are still two main candidates for the compact objects observed in pulsars and gravitational wave (GW) events in binary star mergers. We perform a Bayesian model-agnostic inference of the properties of NSs and QSs by combining multi-messenger data of GW170817, GW190425, PSR J0030+0451, PSR J0740+6620, PSR J1614-2230, PSR J0348+0432 as well as *ab initio* calculations from perturbative quantum chromodynamics and chiral effective field theory. We find the NS scenario is strongly favored against the QS scenario with a Bayes factor of NS over QS  $\mathcal{B}_{\text{QS}}^{\text{NS}} = 11.5$ . In addition, the peak of the squared sound velocity  $c_s^2 \sim 0.5c^2$  around 3.5 times nuclear saturation density  $n_0$  observed in the NS case disappears in the QS case which suggests that the  $c_s^2$  first increases and then saturates at  $c_s^2 \sim 0.5c^2$  above  $\sim 4n_0$ . The sound velocity and trace anomaly are found to approach the conformal limit in the core of heavy NSs with mass  $M \gtrsim 2M_\odot$ , but not in the core of QSs.

*Introduction.*— Understanding the nature of compact stars (CSs) observed in pulsars and gravitational wave (GW) events in binary star mergers is one of fundamental questions in contemporary nuclear physics, astrophysics and cosmology. The baryon number density in the core of CSs can reach several times nuclear saturation density ( $n_0 = 0.16 \text{ fm}^{-3}$ ), making the CSs be ideal laboratories to study the properties of dense nuclear matter and QCD phase diagram at extreme high densities and low temperatures [1–9], which is unaccessible in terrestrial labs. Theoretically, it is still a big challenge to determine the properties of dense nuclear matter at several times of  $n_0$  from *ab initio* QCD calculations due to the complicated nonperturbative feature of QCD [10], and thus the composition inside the CSs is largely unknown. As discussed in Ref. [2], the CSs could be neutron stars (NSs) for which besides the conventional neutrons and protons, some exotic degrees of freedom such as hyperons, meson condensates and even quark matter may appear in the core. A popular alternative for CSs is the self-bound quark stars (QSs) made purely of absolutely stable deconfined quark matter (QM) composed of  $u$ ,  $d$  and  $s$  [11–14] or  $u$  and  $d$  [15–17] quarks with some leptons. The CSs could be even self-bound strangeon stars in a solid state comprised of strangeons (quark-clusters with three-light-flavor symmetry) [18, 19].

Thanks to the fast development in astrophysical observation facilities, significant progress has been made in the last decades for the measurement of CSs. For example, the mass of several heavy pulsars with mass  $M \sim 2M_\odot$  was measured precisely by Shapiro delay [20]. The mass and radius of PSR J0030+0451 with  $M \sim 1.4M_\odot$  and PSR J0740+6620 with  $M \sim 2M_\odot$  were determined simultaneously by NICER via pulse-profile modeling [21–24]. Especially, in recent years, two gravitational wave (GW) events GW170817 [25, 26] and GW190425 [27]

from binary star mergers were reported by the LIGO Scientific and Virgo Collaborations (LVC), which inaugurates a new era of multimessenger astronomy.

Theoretically, *ab initio* calculations of dense matter have also made significant progress in recent years. At the low density limit, chiral effective field theory (ChEFT) [28, 29], which is the low-energy realization of QCD, provides a satisfactory constraint on the equation of state (EOS) of the NS matter up to densities  $n \approx 1 \sim 2n_0$  with controllable uncertainties [30, 31]. At asymptotically high densities with baryon chemical potential of multi GeV, perturbative QCD (pQCD) computations become feasible [32] and provide potential constraints on the EOS of dense matter at intermediate densities inside CSs by combining the results at low densities [33–36]. Based on these state-of-the-art *ab initio* calculations together with the multi-messenger data, it is extremely interesting to perform a comparative study on NSs and QSs, which may provide valuable information on the nature of CSs and the properties of dense matter.

We perform here a Bayesian model-agnostic inference of the properties of NSs and QSs by combining the data on the mass of heavy pulsars with  $M \sim 2M_\odot$  determined by Shapiro delay, the mass and radius of PSR J0030+0451 and PSR J0740+6620 from NICER, the tidal deformabilities of CSs from GW170817 and GW190425 together with *ab initio* calculations from pQCD and ChEFT. We find the current multi-messenger data and constraints from pQCD and ChEFT strongly favor the NS scenario against the QS scenario. In addition, our analyses on the sound velocity and trace anomaly suggest that the conformal limit is violated inside QSs, but reached in the core of heavy NSs with  $M \gtrsim 2M_\odot$ .

*Model-agnostic EOS*— To construct model-agnostic EOSs for NS matter, we adopt the EOS derived from ChEFT at low densities and extrapolate it to high den-

sity to match the pQCD constraints by speed of sound extension approach [37]. In particular, following Ref. [34], in the density region of  $n \in [0.58n_0, 1.1n_0]$ , we choose ‘‘Soft’’, ‘‘Intermediate’’ and ‘‘Stiff’’ EOSs of Ref. [30], and match them to BPS EOS [38] below  $0.58n_0$ . The speed of sound extension [37] is then utilized to obtain EOS of NS matter from  $1.1n_0$  to  $12n_0$ , in which we uniformly sample a sequence of stitching points  $\{(n_i, c_{s,i}^2)\}_{i=1}^N$  ( $n_j > n_k$  for  $j > k$ ). These matching points are then connected using piecewise-linear function to obtain  $c_s^2(n)$  as

$$c_s^2(n) = \frac{(n_{i+1} - n) c_{s,i}^2 + (n - n_i) c_{s,i+1}^2}{n_{i+1} - n_i}, \quad (1)$$

and the EOS of NS matter from  $1.1n_0$  to  $12n_0$  can then be obtained using the fundamental thermodynamic relation (see, e.g., Ref. [36])

$$\mu(n) = \mu_1 \exp \left[ \int_{n_1}^n dn' \frac{c_s^2(n')}{n'} \right], \quad (2)$$

$$\varepsilon(n) = \varepsilon_1 + \int_{n_1}^n dn' \mu(n'), \quad (3)$$

$$p(n) = -\varepsilon(n) + \mu(n)n. \quad (4)$$

We set  $n_1 = 1.1n_0$  and  $n_N = 12n_0$ , and  $c_{s,1}^2$  (also the corresponding chemical potential  $\mu_1$  and energy density  $\varepsilon_1$ ) is fixed at the corresponding value from ChEFT,  $n_i$  ( $i = 2, \dots, N-1$ ) and  $c_{s,i}^2$  ( $i = 2, \dots, N$ ) is uniformly sampled in  $[1.1n_0, 12n_0]$  and  $[0, 1]$  respectively. In the following we use  $N = 6$  and we note that the results just change slightly when  $N$  vary from 5 to 10. The nested sampler *pymultinest* [39] (which is installed in *bilby* [40]) is then used to sample over parameter  $\{(n_i, c_{s,i}^2)\}_{i=1}^N$  and generate posterior distribution.

For QS matter (also for strangeon matter), its EOS is unknown even at low densities, and so we only consider its basic self-bound property with minimum assumption that the pressure becomes to zero at finite baryon number density  $n_1$  corresponding to the QS surface. Assuming  $n_1 > n_0$  and  $n_N = 12n_0$ , we uniformly sample  $n_i$  ( $i = 1, \dots, N-1$ ) ( $n_j > n_k$  for  $j > k$ ) and  $c_{s,i}^2$  ( $i = 1, \dots, N$ ) in  $[n_0, 12n_0]$  and  $[0, 1]$ , respectively. At the same time, we also uniformly sample the chemical potential  $\mu_1$  at  $n_1$  in  $[\mu_{1,\min}, 930]$  MeV with  $\mu_{1,\min} = 500$  MeV, considering the fact that  $\mu_1$  should be less than the binding energy per baryon of the observed stable nuclei (i.e., 930 MeV) to satisfy the absolutely stable condition [11–14]. The energy density at  $n_1$  can then be obtained as  $\varepsilon_1 = \mu_1 n_1$ . The full EOS of QS matter can be then obtained similarly as in the case of NS.

*Bayesian analysis*— We use Bayesian hierarchical model to combine constraints from multiple observations with uncertainties and then make parameter estimate. According to Bayes’ theorem, as discussed in Ref [41, 42], for the given data set  $\vec{d}$  and hypothesis  $\mathcal{H}$ , the posterior

distribution of EOS parameters  $\theta$  can be written as

$$p(\theta|\vec{d}, \mathcal{H}) = \frac{\prod_i \mathcal{L}(d_i|\theta, \mathcal{H}) \pi(\theta|\mathcal{H})}{\mathcal{Z}_{\mathcal{H}}(\vec{d})}, \quad (5)$$

where  $i$  runs over individual constraints and each constraint is independent of each other,  $\pi(\theta|\mathcal{H})$  is the hyper-prior distribution for  $\theta$  and here is chosen as uniform distribution,  $\mathcal{L}(d_i|\theta, \mathcal{H})$  is the likelihood of the EOS parameters under the assumption of  $\mathcal{H}$  for data  $d_i$ , and the  $\mathcal{Z}_{\mathcal{H}}(\vec{d}) \equiv \int \prod_i \mathcal{L}(d_i|\theta, \mathcal{H}) \pi(\theta|\mathcal{H}) d\theta$  is a normalization factor called *evidence* which quantifies how much the hypothesis is preferred by the data. Based on the data set  $\vec{d}$ , the Bayes factor  $\mathcal{B}_{\text{QS}}^{\text{NS}}$  for CSs as NSs against QSs can be obtained as [43]

$$\mathcal{B}_{\text{QS}}^{\text{NS}} = \mathcal{Z}_{\text{NS}}(\vec{d}) / \mathcal{Z}_{\text{QS}}(\vec{d}). \quad (6)$$

In the present Bayesian analyses, we combine the Shapiro delay mass measurements of heavy CSs, the NICER mass-radius of PSR J0030+0451 and PSR J0740+6620 analyzed by Miller *et al.* [21, 22] (Similar to Ref. [44]), the tidal information of GW170817 [25, 26] and GW190425 [27] together with the pQCD constraints at ultra high densities [32, 36, 45, 46] (and ChEFT results for NSs) as our default data set  $\vec{d}_{\text{def}}$ .

For the mass measurements, the prior distribution of CS mass for a given EOS parameter  $\theta$  can be written as [47, 48]  $\pi(m|\theta) = \frac{1_{[M_{\text{low}}, M_{\text{TOV}}(\theta)]}}{M_{\text{TOV}}(\theta) - M_{\text{low}}}$ , where  $M_{\text{low}} = 0.1M_{\odot}$  is the assumed lower bound of the mass of CSs and  $M_{\text{TOV}}(\theta)$  is the maximum mass of static CSs determined by the EOS. For a given mass measurement data  $d_M$ , the likelihood is  $\mathcal{L}(d_M|\theta) = \int dm \mathcal{L}(d_M|m) \pi(m|\theta)$ . We consider here the precise Shapiro delay mass measurement of PSR J1614-2230 [49–51], PSR J0348+0432 [52], PSR J0740+6620 [20] and use Gaussian function  $\mathcal{N}(1.908, 0.016^2)$ ,  $\mathcal{N}(2.01, 0.04^2)$ ,  $\mathcal{N}(2.08, 0.07^2)$  to approximate these mass measurements  $\mathcal{L}(d_M|m)$ , respectively.

Similarly, for the NICER mass-radius measurement data  $d_R$  of PSR J0030+0451 or PSR J0740+6620, the likelihood can be written as  $\mathcal{L}(d_R|\theta) = \int dm \mathcal{L}(d_R|m, R(m, \theta)) \pi(m|\theta)$  and we use Kernel Density Estimation (KDE) to approximate the posterior mass-radius distribution [53, 54]. To avoid double counting, for PSR J0740+6620 [20], we do not use its Shapiro delay mass data if we include its NICER mass-radius data. For PSR J0437-4715, we use 2D Gaussian distribution  $\mathcal{N}([13.6, 1.44]^{\top}, \text{diag}(0.85^2, 0.07^2))$  to approximate its mass-radius joint distribution.

For the measurements of GW events, the likelihood can be written as  $\mathcal{L}(d_{\text{GW}}|\theta) = \int d\omega \mathcal{L}(d_{\text{GW}}|\omega) \pi(\omega|\theta)$  [55], where  $\omega = \{\mathcal{M}_c, q, \Lambda_1, \Lambda_2\}$  and  $\mathcal{L}(d_{\text{GW}}|\omega)$  is the nuisance-marginalized likelihood [41] which has marginalized over extrinsic parameters of the source. With the convention  $m_1 \geq m_2$ , the tidal parameter  $\Lambda_i$

of each compact object could be uniquely determined by the chirp mass  $\mathcal{M}_c$ , mass ratio  $q$ , and EOS parameter  $\theta$ , i.e.  $\Lambda_i(\mathcal{M}_c, q, \theta)$ .

Based on thermodynamic stability and causality, the results from pQCD can be utilized to constrain the EOS at intermediate density region by fully taking advantage of thermodynamic potentials [45]. At a high chemical potential  $\mu_H = 2.6$  GeV (i.e.  $n \approx 40n_0$ ), the uncertainties of thermodynamics quantity could be parameterized by a dimensionless parameter  $X$  and could be expressed by a set  $\vec{\beta}_{\text{pQCD}}(X) = \{p_{\text{pQCD}}(\mu_H, X), n_{\text{pQCD}}(\mu_H, X), \mu_H\}$ . By integrating the uncertainties, one can obtain the corresponding likelihood  $\mathcal{L}(\text{pQCD}|\theta) = \int d\vec{\beta}_H P(\vec{\beta}_H) \mathbf{1}_{[\Delta p_{\min}, \Delta p_{\max}]}(\Delta p)$  [36], with  $\Delta p = p_{\text{pQCD}} - p_L$  and  $p_L$  is the pressure of the last point (i.e.,  $n_N = 12n_0$  here) of interpolated EOS. It should be noted that the  $p_L$  value depends on the EOS at the low density  $n_1$  as well as the sequence of stitching points  $\{(n_i, c_{s,i}^2)\}_{i=1}^N$  in the speed of sound extension.

*Results and discussions*— Using the default data set  $\vec{d}_{\text{def}}$ , we perform Bayesian model-agnostic inference of the properties of NSs and QSs. Firstly, for  $M_{\text{TOV}}$ , our present analyses indicate that it is  $M_{\text{TOV,NS}} = 2.17_{-0.15}^{+0.26} M_{\odot}$  for NSs and  $M_{\text{TOV,QS}} = 2.49_{-0.35}^{+0.47} M_{\odot}$  for QSs in 90% credible interval (CI), indicating the QSs would have a significantly larger  $M_{\text{TOV}}$  than the NSs. The  $M_{\text{TOV,NS}} = 2.17_{-0.15}^{+0.26} M_{\odot}$  is in nice agreement with the value of  $2.18_{-0.13}^{+0.27} M_{\odot}$  estimated recently by taking advantage of the various structures sampling by a single-layer feed-forward neural network model embedded in the Bayesian nonparametric inference [56], implying our present result is independent of the detailed realization of the model-agnostic EOSs.

Secondly, for the radius  $R_{1.4}$  of CSs with canonical mass of  $1.4M_{\odot}$ , its value is estimated to be  $R_{1.4,\text{NS}} = 12.44_{-0.71}^{+0.74}$  km for NSs and  $R_{1.4,\text{QS}} = 11.41_{-0.61}^{+0.64}$  km for QSs in 90% CI, suggesting NSs have a larger  $R_{1.4}$  than QSs.  $R_{1.4,\text{NS}} = 12.44_{-0.71}^{+0.74}$  km well agrees with  $R_{1.4} = 12.42_{-0.99}^{+0.52}$  km (95% CI) reported in Ref. [57] where an ensemble of EOSs is generated in advance and weight each EOS according to the likelihood. Our result on  $R_{1.4,\text{NS}}$  is also consistent with  $R_{1.4} = 11.98_{-0.40}^{+0.35}$  (90% CI) [58] obtained recently by combining all the EOS-sensitive observations, including data of the kilonovae and the GRB afterglow. In addition, though different methods are adopted to construct EOS, our result on  $R_{1.4,\text{NS}}$  is in agreement with previous work [44, 59–66] within the uncertainty. For the case of QSs, our result also agrees with  $R_{1.4} = 11.50_{-0.55}^{+0.52}$  km obtained by Miao *et al.* [67] within the MIT bag model.

Thirdly, the tidal deformability  $\Lambda_{1.4}$  of a  $1.4M_{\odot}$  CS is estimated to be  $\Lambda_{1.4,\text{NS}} = 504_{-174}^{+223}$  for NSs and  $\Lambda_{1.4,\text{QS}} = 642_{-204}^{+260}$  for QSs in 90% CI, and thus QSs would have a significantly larger  $\Lambda_{1.4}$  than NSs. The obtained  $\Lambda_{1.4,\text{NS}}$  nicely agrees with the result  $507_{-242}^{+234}$  in Ref. [60]

where the Gaussian processes are applied to construct the model-independent EOSs. Our result on  $\Lambda_{1.4,\text{QS}}$  is also consistent with  $\Lambda_{1.4} = 650_{-190}^{+230}$  obtained in Ref. [67] within the MIT bag model.

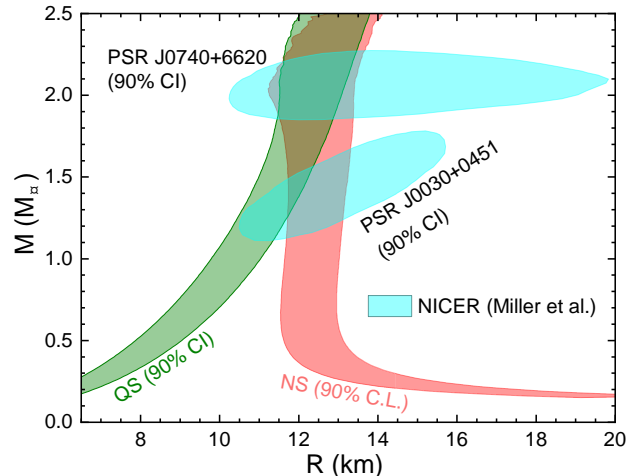


FIG. 1. Posterior distribution of radius of NSs and QSs at different masses (90% CI). The NICER mass-radius posterior distributions (90% CI) of PSR J0030+0451 [21] and PSR J0740+6620 [22] are also shown for comparison.

The above discussions indicate that the NS and QS scenarios lead to different predictions of  $M_{\text{TOV}}$ ,  $R_{1.4}$  and  $\Lambda_{1.4}$  for CSs. To assess the preference of the NS and QS hypotheses in the description of the current multi-messenger data under the constraints from pQCD and ChEFT, we evaluate the Bayes factor of NS over QS and find  $\mathcal{B}_{\text{QS}}^{\text{NS}} = 11.5$ . This value of  $\mathcal{B}_{\text{QS}}^{\text{NS}}$  means that the NS hypothesis for CSs is strongly preferred against the QS hypothesis according to the interpretation of Bayes factor, i.e., the  $\mathcal{B}_{H_0}^{H_1} \in [10, 30]$  indicates strong evidence for hypothesis  $H_1$  [68]. To see the main reason leading to the large value of  $\mathcal{B}_{\text{QS}}^{\text{NS}} = 11.5$ , we calculate the  $\mathcal{B}_{\text{QS}}^{\text{NS}}$  by removing individually the data from the default data set  $\vec{d}_{\text{def}}$ , and we find the value of  $\mathcal{B}_{\text{QS}}^{\text{NS}}$  changes to 16.1, 5.1, 10.6, 12.4 and 1.3 by removing the data/constraints of pQCD, GW170817, GW190425, PSR J0740+6620 and PSR J0030+0451, respectively. The large value of  $\mathcal{B}_{\text{QS}}^{\text{NS}} = 11.5$  is thus mainly due to the constraint from PSR J0030+0451, and next from GW170817. To see more clearly the influence of PSR J0030+0451, we show in Fig. 1 the 90% CI of radius at different masses for NSs and QSs. It is seen that the NS hypothesis can indeed describe the NICER measurements of PSR J0030+0451 much better than the QS hypothesis as the latter just marginally overlaps with the NICER mass-radius of PSR J0030+0451 where the probability density is relatively low. Therefore, our results suggest that the multi-messenger data prefer CSs as NSs over QSs, implying the conjecture of QM (as well as the strangeon matter) as the true ground state of QCD mat-

ter [11–14] is disfavored. This may provide a natural explanation on the fact that there is so far no definite evidence for the existence of strangelet-like exotic objects after decades experimental and observational searching (See, e.g., Refs. [69, 70]).

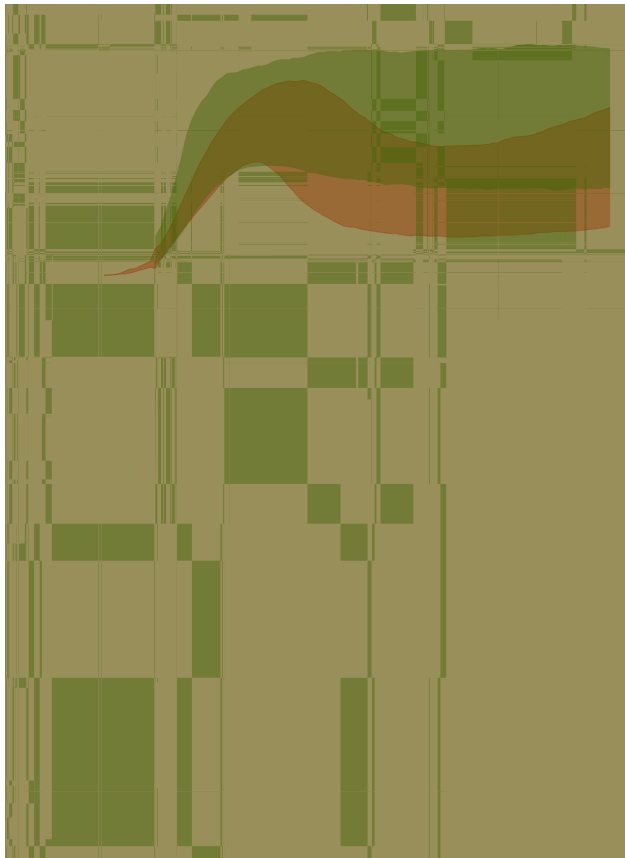


FIG. 2. Posterior distributions (68% CI) and the corresponding median values for squared speed of sound  $c_s^2$  (a), pressure  $p$  (b) and trace anomaly  $\Delta$  (c) of NS matter and QS matter as functions of baryon number density.

The sound velocity  $c_s$  is an important quantity to feature the EOS of density matter. Shown in Fig. 2(a) is the 68% CI of  $c_s^2$  as a function of baryon density for NS matter and QS matter. One sees the squared speed of sound  $c_{s,NS}^2$  for NS matter first increases with baryon density and reaches a peak value of  $c_{s,NS,max}^2 \sim 0.5c^2$  ( $c$  is the speed of light in vacuum) around  $n \approx 3.5n_0$  (i.e.,  $n_{pk,NS} = 0.55_{-0.14}^{+0.19} \text{ fm}^{-3}$ ), then decreases and approaches the conformal limit  $c^2/3$  above  $n \approx 4.5n_0$ . This peak structure may be related to the quarkyonic matter [71] or the high density behavior of the symmetry energy [72]. It is interesting to mention that according to percolation theory, the critical density that nucleons begin overlap with each other is estimated to be  $0.57_{-0.09}^{+0.12} \text{ fm}^{-3}$  [73], very close to the  $n_{pk,NS}$ . We have checked that the peak structure will disappear if the pQCD constraint is removed from  $\vec{d}_{def}$ . Furthermore, if the constraints

of heavy CSs with  $M \approx 2M_\odot$  are excluded from  $\vec{d}_{def}$ , the  $c_{s,NS}^2$  will increase monotonously until  $12n_0$ . Therefore, the constraints from pQCD and heavy CSs with  $M \approx 2M_\odot$  are necessary conditions for the sound velocity peak structure in NS matter.

In contrast to  $c_{s,NS}^2$ , it is interesting to see from Fig. 2(a) that the squared speed of sound  $c_{s,QS}^2$  for QS matter first increases with baryon density and then essentially saturates at about  $0.5c^2$  above  $n \sim 4n_0$ . Therefore, the peak structure is not present in  $c_{s,QS}^2$  although the constraints of pQCD and heavy CSs with  $M \approx 2M_\odot$  are both considered. This feature clearly shows that the pQCD limits on the EOS and  $c_s^2$  of dense matter at intermediate densities inside CSs significantly depends on the input EOS at low densities. Indeed, the low density EOS is very different for NS and QS matters, as illustrated in Fig. 2(b) where the 68% CI of pressure as a function of baryon density is displayed for NS and QS matters. One sees from Fig. 2(b) that the pressure of NS matter is well constrained by BPS EOS and ChEFT below  $1.1n_0$  but the pressure of QS matter around  $n_0$  rapidly drops to zero due to absolutely stable condition although with large uncertainties. Quantitatively, the energy per baryon  $\mu_1$  and the number density  $n_1$  at zero pressure point of QS matter are estimated to be [654, 812] MeV and  $[0.24, 0.35] \text{ fm}^{-3}$  (68% CI), respectively.

Very recently, the trace anomaly normalized by the energy density, i.e.,  $\Delta = 1/3 - p/\epsilon$ , is proposed as a new measure of conformality [74]. Shown in Fig. 2(c) is the 68% CI of the (normalized) trace anomaly  $\Delta$  as a function of baryon density for NS and QS matters. One sees the  $\Delta$  for NS matter first decreases with baryon density and then essentially approaches the conformal limit  $\Delta = 0$  above  $n \approx 4.5n_0$ . On the other hand, for QS matter, the  $\Delta$  decreases monotonously and becomes negative above  $n \approx 5n_0$ . As pointed out in Ref. [74], the sound velocity can be decomposed into the derivative and the nonderivative terms in terms of  $\Delta$ , i.e.,  $c_s^2/c^2 = 1/3 - \Delta - \epsilon d\Delta/d\epsilon$ , and the sound velocity peak observed in NS matter can be attributed to the derivative term from  $\Delta$ . In addition, our results indicate while the NS matter seems to obey the conjecture [74] that the matter part of the trace anomaly is positive definite, the QS matter violates it.

Furthermore, we note that the central density in  $2M_\odot$  and maximum mass ( $M = 2.17_{-0.15}^{+0.26} M_\odot$ ) NS are estimated to be  $n_{c,NS,2M} = 0.56_{-0.10}^{+0.14} \text{ fm}^{-3}$  and  $n_{c,NS,max} = 0.90_{-0.12}^{+0.11} \text{ fm}^{-3}$ , respectively. The corresponding values for QS are  $n_{c,QS,2M} = 0.54_{-0.09}^{+0.11} \text{ fm}^{-3}$  and  $n_{c,QS,max} = 0.97_{-0.14}^{+0.16} \text{ fm}^{-3}$ , respectively. These results imply that the conformal symmetry may be restored in the core of heavy NSs with  $M \gtrsim 2M_\odot$ , consistent with the conclusion obtained recently from other groups [73–75].

*Conclusion.*— Based on Bayesian model-agnostic inference of the properties of NSs and QSs by combining the multi-messenger data and *ab initio* calculations

from pQCD and ChEFT, we find that the NS scenario is strongly favored against the QS scenario for the CSs, and the NS and QS matters display rather different density behaviors of sound velocity and trace anomaly. Our finding sheds light on the nature of CSs observed in pulsars and gravitational wave events in binary star mergers and provides valuable information on the properties of dense matter inside CSs.

*Acknowledgments.*— The authors would like to thank Tyler Gorda, Sohpia Han, Aleks Kurkela, Ang Li, Yifeng Sun, Renxin Xu, Zhen Zhang and Zhenyu Zhu for useful discussions. This work was supported by the National SKA Program of China No. 2020SKA0120300 and the National Natural Science Foundation of China under Grant Nos. 12235010 and 11625521. The computations in this paper were run on the Siyuan-1 cluster supported by the Center for High Performance Computing at Shanghai Jiao Tong University.

---

\* Corresponding author; [lwchen@sjtu.edu.cn](mailto:lwchen@sjtu.edu.cn)

- [1] J. M. Lattimer and M. Prakash, *Science* **304**, 536 (2004), [arXiv:astro-ph/0405262](https://arxiv.org/abs/astro-ph/0405262).
- [2] F. Weber, *Progress in Particle and Nuclear Physics* **54**, 193 (2005).
- [3] M. G. Alford, A. Schmitt, K. Rajagopal, and T. Schäfer, *Rev. Mod. Phys.* **80**, 1455 (2008), [arXiv:0709.4635](https://arxiv.org/abs/0709.4635) [hep-ph].
- [4] K. Fukushima and T. Hatsuda, *Rept. Prog. Phys.* **74**, 014001 (2011), [arXiv:1005.4814](https://arxiv.org/abs/1005.4814) [hep-ph].
- [5] G. Baym, T. Hatsuda, T. Kojo, P. D. Powell, Y. Song, and T. Takatsuka, *Rept. Prog. Phys.* **81**, 056902 (2018), [arXiv:1707.04966](https://arxiv.org/abs/1707.04966) [astro-ph.HE].
- [6] D. Blaschke and N. Chamel, *Astrophys. Space Sci. Libr.* **457**, 337 (2018), [arXiv:1803.01836](https://arxiv.org/abs/1803.01836) [nucl-th].
- [7] G. F. Burgio, H. J. Schulze, I. Vidana, and J. B. Wei, *Prog. Part. Nucl. Phys.* **120**, 103879 (2021), [arXiv:2105.03747](https://arxiv.org/abs/2105.03747) [nucl-th].
- [8] B.-A. Li, B.-J. Cai, W.-J. Xie, and N.-B. Zhang, *Universe* **7**, 182 (2021), [arXiv:2105.04629](https://arxiv.org/abs/2105.04629) [nucl-th].
- [9] A. Sedrakian, J.-J. Li, and F. Weber, *Prog. Part. Nucl. Phys.* **131**, 104041 (2023), [arXiv:2212.01086](https://arxiv.org/abs/2212.01086) [nucl-th].
- [10] N. Brambilla *et al.*, *Eur. Phys. J. C* **74**, 2981 (2014), [arXiv:1404.3723](https://arxiv.org/abs/1404.3723) [hep-ph].
- [11] A. R. Bodmer, *Phys. Rev. D* **4**, 1601 (1971).
- [12] E. Witten, *Phys. Rev. D* **30**, 272 (1984).
- [13] H. Terazawa, *J. Phys. Soc. Jap.* **58**, 3555 (1989).
- [14] E. Farhi and R. L. Jaffe, *Phys. Rev. D* **30**, 2379 (1984).
- [15] B. Holdom, J. Ren, and C. Zhang, *Phys. Rev. Lett.* **120**, 222001 (2018), [arXiv:1707.06610](https://arxiv.org/abs/1707.06610) [hep-ph].
- [16] T. Zhao, W. Zheng, F. Wang, C.-M. Li, Y. Yan, Y.-F. Huang, and H.-S. Zong, *Phys. Rev. D* **100**, 043018 (2019), [arXiv:1904.09744](https://arxiv.org/abs/1904.09744) [nucl-th].
- [17] Z. Cao, L.-W. Chen, P.-C. Chu, and Y. Zhou, *Phys. Rev. D* **106**, 083007 (2022), [arXiv:2009.00942](https://arxiv.org/abs/2009.00942) [astro-ph.HE].
- [18] R.-X. Xu, *Astrophys. J. Lett.* **596**, L59 (2003), [arXiv:astro-ph/0302165](https://arxiv.org/abs/astro-ph/0302165).
- [19] R. Xu, *Sci. China Phys. Mech. Astron.* **61**, 109531 (2018), [arXiv:1802.04465](https://arxiv.org/abs/1802.04465) [astro-ph.HE].
- [20] E. Fonseca *et al.*, *Astrophys. J. Lett.* **915**, L12 (2021), [arXiv:2104.00880](https://arxiv.org/abs/2104.00880) [astro-ph.HE].
- [21] M. C. Miller *et al.*, *Astrophys. J. Lett.* **887**, L24 (2019), [arXiv:1912.05705](https://arxiv.org/abs/1912.05705) [astro-ph.HE].
- [22] M. C. Miller *et al.*, *Astrophys. J. Lett.* **918**, L28 (2021), [arXiv:2105.06979](https://arxiv.org/abs/2105.06979) [astro-ph.HE].
- [23] T. E. Riley *et al.*, *Astrophys. J. Lett.* **887**, L21 (2019), [arXiv:1912.05702](https://arxiv.org/abs/1912.05702) [astro-ph.HE].
- [24] T. E. Riley *et al.*, *Astrophys. J. Lett.* **918**, L27 (2021), [arXiv:2105.06980](https://arxiv.org/abs/2105.06980) [astro-ph.HE].
- [25] B. P. Abbott *et al.* (LIGO Scientific, Virgo), *Phys. Rev. Lett.* **119**, 161101 (2017), [arXiv:1710.05832](https://arxiv.org/abs/1710.05832) [gr-qc].
- [26] B. P. Abbott *et al.* (LIGO Scientific, Virgo), *Phys. Rev. X* **9**, 011001 (2019), [arXiv:1805.11579](https://arxiv.org/abs/1805.11579) [gr-qc].
- [27] B. P. Abbott *et al.* (LIGO Scientific, Virgo), *Astrophys. J. Lett.* **892**, L3 (2020), [arXiv:2001.01761](https://arxiv.org/abs/2001.01761) [astro-ph.HE].
- [28] J. W. Holt, M. Rho, and W. Weise, *Phys. Rept.* **621**, 2 (2016), [arXiv:1411.6681](https://arxiv.org/abs/1411.6681) [nucl-th].
- [29] C. Drischler, J. W. Holt, and C. Wellenhofer, *Ann. Rev. Nucl. Part. Sci.* **71**, 403 (2021), [arXiv:2101.01709](https://arxiv.org/abs/2101.01709) [nucl-th].
- [30] K. Hebeler, J. M. Lattimer, C. J. Pethick, and A. Schwenk, *Astrophys. J.* **773**, 11 (2013), [arXiv:1303.4662](https://arxiv.org/abs/1303.4662) [astro-ph.SR].
- [31] C. Wellenhofer, J. W. Holt, and N. Kaiser, *Phys. Rev. C* **92**, 015801 (2015), [arXiv:1504.00177](https://arxiv.org/abs/1504.00177) [nucl-th].
- [32] T. Gorda, A. Kurkela, R. Paatelainen, S. Säppi, and A. Vuorinen, *Phys. Rev. Lett.* **127**, 162003 (2021), [arXiv:2103.05658](https://arxiv.org/abs/2103.05658) [hep-ph].
- [33] E. Annala, T. Gorda, A. Kurkela, and A. Vuorinen, *Phys. Rev. Lett.* **120**, 172703 (2018), [arXiv:1711.02644](https://arxiv.org/abs/1711.02644) [astro-ph.HE].
- [34] E. Annala, T. Gorda, A. Kurkela, J. Nättilä, and A. Vuorinen, *Nature Phys.* **16**, 907 (2020), [arXiv:1903.09121](https://arxiv.org/abs/1903.09121) [astro-ph.HE].
- [35] E. Annala, T. Gorda, E. Katerini, A. Kurkela, J. Nättilä, V. Paschalidis, and A. Vuorinen, *Phys. Rev. X* **12**, 011058 (2022), [arXiv:2105.05132](https://arxiv.org/abs/2105.05132) [astro-ph.HE].
- [36] T. Gorda, O. Komoltsev, and A. Kurkela, *Astrophys. J.* **950**, 107 (2023), [arXiv:2204.11877](https://arxiv.org/abs/2204.11877) [nucl-th].
- [37] I. Tews, J. Carlson, S. Gandolfi, and S. Reddy, *Astrophys. J.* **860**, 149 (2018), [arXiv:1801.01923](https://arxiv.org/abs/1801.01923) [nucl-th].
- [38] G. Baym, C. Pethick, and P. Sutherland, *Astrophys. J.* **170**, 299 (1971).
- [39] J. Buchner, A. Georgakakis, K. Nandra, L. Hsu, C. Rangel, M. Brightman, A. Merloni, M. Salvato, J. Donley, and D. Kocevski, *Astron. Astrophys.* **564**, A125 (2014), [arXiv:1402.0004](https://arxiv.org/abs/1402.0004) [astro-ph.HE].
- [40] G. Ashton *et al.*, *Astrophys. J. Suppl.* **241**, 27 (2019), [arXiv:1811.02042](https://arxiv.org/abs/1811.02042) [astro-ph.IM].
- [41] F. Hernandez Vivanco, R. Smith, E. Thrane, and P. D. Lasky, *Mon. Not. Roy. Astron. Soc.* **499**, 5972 (2020), [arXiv:2008.05627](https://arxiv.org/abs/2008.05627) [astro-ph.HE].
- [42] E. Thrane and C. Talbot, *Publ. Astron. Soc. Austral.* **36**, e010 (2019), [Erratum: *Publ. Astron. Soc. Austral.* **37**, e036 (2020)], [arXiv:1809.02293](https://arxiv.org/abs/1809.02293) [astro-ph.IM].
- [43] H. Jeffreys, *Theory of Probability* (Oxford University Press, New York, 1961).
- [44] S. Huth *et al.*, *Nature* **606**, 276 (2022), [arXiv:2107.06229](https://arxiv.org/abs/2107.06229) [nucl-th].
- [45] O. Komoltsev and A. Kurkela, *Phys. Rev. Lett.* **128**, 202701 (2022), [arXiv:2111.05350](https://arxiv.org/abs/2111.05350) [nucl-th].
- [46] Likelihood function of QCD, <https://github.com/OKomoltsev/QCD-likelihood-function>.

- [47] P. Landry, R. Essick, and K. Chatziioannou, *Phys. Rev. D* **101**, 123007 (2020), [arXiv:2003.04880 \[astro-ph.HE\]](#).
- [48] B. Biswas, *Astrophys. J.* **926**, 75 (2022), [arXiv:2106.02644 \[astro-ph.HE\]](#).
- [49] P. Demorest, T. Pennucci, S. Ransom, M. Roberts, and J. Hessels, *Nature* **467**, 1081 (2010), [arXiv:1010.5788 \[astro-ph.HE\]](#).
- [50] E. Fonseca *et al.*, *Astrophys. J.* **832**, 167 (2016), [arXiv:1603.00545 \[astro-ph.HE\]](#).
- [51] Z. Arzoumanian *et al.* (NANOGrav), *Astrophys. J. Suppl.* **235**, 37 (2018), [arXiv:1801.01837 \[astro-ph.HE\]](#).
- [52] J. Antoniadis *et al.*, *Science* **340**, 6131 (2013), [arXiv:1304.6875 \[astro-ph.HE\]](#).
- [53] NICER PSR J0030+0451 Illinois-Maryland MCMC Samples, J0030\_3spot\_RM.txt, <https://zenodo.org/record/3473466>.
- [54] NICER PSR J0740+6620 Illinois-Maryland MCMC Samples, NICER+XMM\_J0740\_RM.txt, <https://zenodo.org/record/4670689>.
- [55] F. Hernandez Vivanco, R. Smith, E. Thrane, P. D. Lasky, C. Talbot, and V. Raymond, *Phys. Rev. D* **100**, 103009 (2019), [arXiv:1909.02698 \[gr-qc\]](#).
- [56] M.-Z. Han, Y.-J. Huang, S.-P. Tang, and Y.-Z. Fan, *Sci. Bull.* **68**, 913 (2023), [arXiv:2207.13613 \[astro-ph.HE\]](#).
- [57] S. Altiparmak, C. Ecker, and L. Rezzolla, *Astrophys. J. Lett.* **939**, L34 (2022), [arXiv:2203.14974 \[astro-ph.HE\]](#).
- [58] P. T. H. Pang *et al.*, (2022), [arXiv:2205.08513 \[astro-ph.HE\]](#).
- [59] P. T. H. Pang, I. Tews, M. W. Coughlin, M. Bulla, C. Van Den Broeck, and T. Dietrich, *Astrophys. J.* **922**, 14 (2021), [arXiv:2105.08688 \[astro-ph.HE\]](#).
- [60] I. Legred, K. Chatziioannou, R. Essick, S. Han, and P. Landry, *Phys. Rev. D* **104**, 063003 (2021), [arXiv:2106.05313 \[astro-ph.HE\]](#).
- [61] B. Biswas, P. Char, R. Nandi, and S. Bose, *Phys. Rev. D* **103**, 103015 (2021), [arXiv:2008.01582 \[astro-ph.HE\]](#).
- [62] Y. Li, H. Chen, D. Wen, and J. Zhang, *Eur. Phys. J. A* **57**, 31 (2021), [arXiv:2008.02955 \[nucl-th\]](#).
- [63] M.-Z. Han, J.-L. Jiang, S.-P. Tang, and Y.-Z. Fan, *Astrophys. J.* **919**, 11 (2021), [arXiv:2103.05408 \[hep-ph\]](#).
- [64] T. Dietrich, M. W. Coughlin, P. T. H. Pang, M. Bulla, J. Heinzel, L. Issa, I. Tews, and S. Antier, *Science* **370**, 1450 (2020), [arXiv:2002.11355 \[astro-ph.HE\]](#).
- [65] J.-L. Jiang, S.-P. Tang, Y.-Z. Wang, Y.-Z. Fan, and D.-M. Wei, *Astrophys. J.* **892**, 1 (2020), [arXiv:1912.07467 \[astro-ph.HE\]](#).
- [66] D. Radice and L. Dai, *Eur. Phys. J. A* **55**, 50 (2019), [arXiv:1810.12917 \[astro-ph.HE\]](#).
- [67] Z. Miao, J.-L. Jiang, A. Li, and L.-W. Chen, *Astrophys. J. Lett.* **917**, L22 (2021), [arXiv:2107.13997 \[astro-ph.HE\]](#).
- [68] M. D. Lee and E.-J. Wagenmakers, *Bayesian Cognitive Modeling* (Cambridge University Press, Cambridge, England, 2014).
- [69] B. I. Abelev *et al.* (STAR), *Phys. Rev. C* **76**, 011901 (2007), [arXiv:nucl-ex/0511047](#).
- [70] K. Han (LSSS), *J. Phys. G* **36**, 064048 (2009), [arXiv:0812.3885 \[nucl-ex\]](#).
- [71] L. McLerran and S. Reddy, *Phys. Rev. Lett.* **122**, 122701 (2019), [arXiv:1811.12503 \[nucl-th\]](#).
- [72] N.-B. Zhang and B.-A. Li, *Eur. Phys. J. A* **59**, 86 (2023), [arXiv:2208.00321 \[nucl-th\]](#).
- [73] M. Marczenko, L. McLerran, K. Redlich, and C. Sasaki, *Phys. Rev. C* **107**, 025802 (2023), [arXiv:2207.13059 \[nucl-th\]](#).
- [74] Y. Fujimoto, K. Fukushima, L. D. McLerran, and M. Praszalowicz, *Phys. Rev. Lett.* **129**, 252702 (2022), [arXiv:2207.06753 \[nucl-th\]](#).
- [75] E. Annala, T. Gorda, J. Hirvonen, O. Komoltsev, A. Kurkela, J. Nättilä, and A. Vuorinen, (2023), [arXiv:2303.11356 \[astro-ph.HE\]](#).